Journal of Thermal Analysis and Calorimetry (2018) 133:1589–1596
https://doi.org/10.1007/s10973-018-7180-4

Thermodynamic properties of the $NdBr_3$–MBr binary systems (M = Na, K)

Yassine Bounouri[1] · Madjid Berkani[1] · Abdelmalek Zamouche[1] · Anna Dańczak[2] · Ida Chojnacka[2] · Leszek Rycerz[2]

Received: 27 December 2017 / Accepted: 8 March 2018 / Published online: 31 March 2018

Abstract
Phase equilibria in the $NdBr_3$–MBr binary systems (M = Na, K) were established by differential scanning calorimetry. The system with NaBr is a simple eutectic system with two compounds that decompose in the solid state ($NaNdBr_4$ at 603 K and Na_3NdBr_6 at 580 K). In the system with KBr, three stoichiometric compounds exist. First (K_3NdBr_6) is formed from KBr and K_2NdBr_5 at 680 K and melts congruently at 918 K. Second (KNd_2Br_7) melts congruently at 814 K. Third compound (K_2NdBr_5) melts incongruently at 822 K.

Keywords Phase diagrams · Phase transitions · Thermal analysis · Enthalpy · DSC

Introduction

Lanthanide bromides and iodides have been used in various technological applications. They are attractive components for doses in high-intensity discharge lamps and new highly efficient light sources with energy-saving features [1–9]. When they are combined with other metal halides, they can be applied in designing light sources with high efficacy and good color rendition. Photoluminescence and photo-stimulated luminescence of lanthanide-doped bromide materials have made research targeted at commercial X-ray storage phosphors [10] more intense lately, while laser activity in lanthanide-doped bromide host crystals has been achieved recently [11–13]. The scintillation properties of lanthanide halides determine their application as highly sensitive radiation detectors [14, 15]. As it was pointed out in a recent review [16], the properties of many rare-earth halides are poorly characterized and the bromides have received even less attention than chlorides and iodides. However, the rare-earth bromides importance is certainly not reflected in the amount of available experimental information on the thermodynamic characterization of both condensed and vapor phases. Only a few works concerning phase diagrams of $LnBr_3$–MBr binary systems (Ln = lanthanide, M = alkali metal) have been reported in the literature [17–21]. The phase diagrams were presented in a graphic form only, without numerical data. In addition, significant discrepancies can be found between the data reported by different authors. For example, Vogel [17] claims an existence of only two compounds (Cs_3SmBr_6 and $CsSm_2Br_7$) in the $SmBr_3$–CsBr system, whereas according to Blachnik and Jaeger-Kasper's investigation [18] four compounds (Cs_3SmBr_6, $Cs_3Sm_2Br_9$, Cs_2SmBr_5 and $CsSm_2Br_7$) are present in this system. The phase diagram of $TmBr_3$–RbBr given by Molodkin et al. is very doubtful [21], which, contrary to all the other lanthanide bromide–rubidium bromide systems, was found to be a simple eutectic system. Another example of discrepancies is the $LaBr_3$–CsBr binary phase diagram. According to Vogel [17], two compounds (Cs_3LaBr_6 and $CsLa_4Br_{13}$) exist in it, whereas investigation of Seifert and Yuan [22] performed later by DTA method showed an existence of three compounds (Cs_3LaBr_6, Cs_2LaBr_5 and $CsLa_2Br_7$), only one of which had the same stoichiometry as the one reported in the older work [17]. The same discrepancies concern the

✉ Leszek Rycerz
leszek.rycerz@pwr.edu.pl

[1] Laboratoire de Physico-chimie des Matériaux et Catalyse, Faculté des Sciences Exactes, Université de Bejaia, Targa ouzemmour, 06000 Béjaïa, Algeria

[2] Chemical Metallurgy Group, Department of Chemistry, Wroclaw University of Science and Technology, Wybrzeze Wyspianskiego 27, 50-370 Wroclaw, Poland

$NdBr_3$–KBr system. According to Blachnik and Jaeger-Kasper [18], three compounds (K_3NdBr_6, K_3NdBr_6, K_2NdBr_5 and KNd_2Br_7 and KNd_2Br_7) are present in this system. Two of them melt congruently (K_3NdBr_6 and KNd_2Br_7), and third (K_2NdBr_5) melts incongruently. However, later literature data [23] are completely different. They suggest an existence of only two compounds (KNd_2Br_7 and K_3NdBr_6). In addition, their behavior is completely different. First of them decomposes in the solid state, and second melts incongruently. Therefore, we decided to reinvestigate this system in order to clarify the situation. In addition, we have investigated also phase equilibria in the $NdBr_3$–NaBr binary system. These investigations are part of our general research program targeted at determination of unknown and verification of existing phase diagrams of lanthanide halide–alkali metal halide systems. Previously, we reported the results of investigations concerning the phase diagrams of the $CeBr_3$–MBr (M = alkali metal) [24–28], $PrBr_3$–MBr [29–32], $TbBr_3$–MBr [33–35] and $DyBr_3$–MBr [36–39] binary systems. The present paper is a continuation of this ongoing extensive program. It presents the phase equilibria in the $NdBr_3$–MBr (M = Na, K) binaries. Some preliminary results concerning $NdBr_3$–KBr system were presented during the conference [40]; however, they were never published.

Experimental

Chemicals and samples preparation

Neodymium(III) bromide used in the investigation was prepared by the so-called wet method [39] from the neodymium(III) oxide (Sigma-Aldrich, min. 99.9%). The main steps of this synthesis included dissolution of neodymium oxide in hot concentrated hydrobromic acid (Fluka > 48%), crystallization of hydrated neodymium bromide, dehydration and melting of anhydrous bromide in the presence of excess ammonium bromide as well as purification of neodymium bromide by distillation under reduced pressure (10^{-5} Pa) in a quartz ampoule at 1150 K. $NdBr_3$ prepared in this way was of high purity (minimum 99.9%). Chemical analysis was performed by complexometric (neodymium) and mercurimetric (bromine) methods. The results were as follows: Nd, 37.55 ± 0.15% (37.57% theoretical), and Br, 62.45 ± 0.11% (62.43% theoretical).

Alkali metal bromides (NaBr and KBr) were Merck Suprapur reagents (minimum 99.9%). Before use, they were progressively heated up to fusion under gaseous HBr atmosphere. Excess of HBr was then removed from the melt by argon bubbling. All chemicals were handled inside a high-purity argon atmosphere in a glove box (water content < 2 ppm).

The $NdBr_3$ and KBr or NaBr mixtures (in appropriate proportions weighed with precision of about 1 mg) were prepared in vacuum-sealed quartz ampoules and melted in electric furnace at 1150 K. After homogenization and solidification, these samples were ground in an agate mortar in a glove box. Different compositions prepared in this way were used both in phase diagram and in electrical conductivity measurements.

Measurements

Phase equilibria in the $NdBr_3$–MBr (M = Na, K) systems were investigated with a Setaram LABSYS evo 1600 differential scanning calorimeter. Experimental samples (200–500 mg) were stored in vacuum-sealed quartz ampoules. Experiments were conducted at heating and cooling rates of 5 K min^{-1}. Prior to measurements, the apparatus was calibrated by measurements of temperatures and enthalpies of phase transitions of standard substances [In, Sn, Zn, Sb and Ag metals of high purity (99.999%)]. The results obtained were used in calculation of temperature and enthalpy correction coefficients, which were introduced into apparatus software. Subsequently, apparatus was tested with high-purity metals and results obtained showed that the maximum relative experimental error on enthalpy of phase transition did not exceed 1%. Temperature was measured with precision ± 1 K.

Results and discussion

$NdBr_3$–NaBr phase diagram

DSC investigations, performed on 21 samples with different compositions with heating and cooling rates of 5 K min^{-1}, yielded both the corresponding temperature and enthalpy values. Due to a supercooling effect, all the experimental temperature and enthalpy values reported in this work were determined from heating curves. In all heating runs, the maximum at the highest temperature corresponds to the liquidus temperature; in all the other cases, onset temperature (T_{ons}) was assumed as the effect temperature. The analysis of the DSC curves was performed with Setaram Calisto software, which also allowed us to separate overlapping peaks.

Some characteristic DSC heating curves are presented in Fig. 1. In the whole composition range, three endothermic peaks were present in all the heating curves. The effect at the highest temperature corresponds, as stated previously, to the liquidus temperature. The second peak also observed in all the samples at 645 K (a mean value from all the

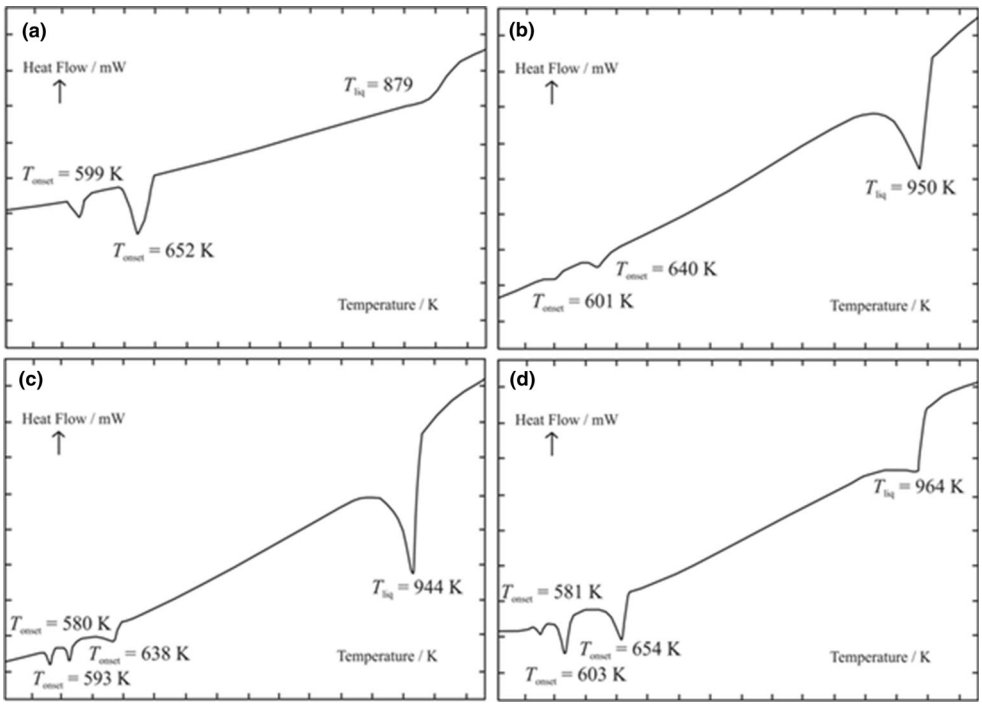

Fig. 1 DSC heating curves for $NaBr–NdBr_3$ mixtures of different compositions: **a** x $NdBr_3$ = 0.751, **b** x $NdBr_3$ = 0.950, **c** x $NdBr_3$ = 0.050, **d** x = 0.100

samples) can be related to the $NaBr–NdBr_3$ eutectic. The eutectic contribution to the enthalpy of fusion was determined, and it is plotted *versus* composition in Fig. 2c. This so-called Tammann construction makes it possible to accurately estimate the eutectic composition from the intercept of the two linear parts in Fig. 2c, as x ($NdBr_3$) = 0.443. The mixture with eutectic composition melts with enthalpy $\Delta_{fus}H_m$ = 14.9 kJ mol^{-1}.

The third effect, at 603 K (a mean value from the measurements), is also observable in all the curves. The Tammann diagram was constructed for this effect (Fig. 2b). The intercept of the two linear parts in this diagram takes place at $x(NdBr_3)$ = 0.485, thus suggesting the existence of a compound with stoichiometry $NaNdBr_4$. This compound decomposes in the solid state with enthalpy of 8.4 kJ mol^{-1}.

In the composition range $0 < x \leq 0.500$, where x is a mole fraction of $NdBr_3$, an additional effect at about 580 K was observed on the DSC curves (Fig. 1c, d). The Tammann diagram for this effect gives value $x(NdBr_3)$ = 0.236, which corresponds to the stoichiometry Na_3NdBr_6 quite well. Accordingly, this effect can be ascribed to decomposition of Na_3NdBr_6 in the solid state.

All the experimental results are listed in Table 1, and the phase diagram is shown in Fig. 3.

A graphic form of the phase diagram reported by Vogel [17] was the only experimental literature information about this system. According to this information, the system under investigation is an eutectic system with an additional effect taking place in the solid phase at 591 K. The nature of this effect was not explained by author. Our finding for the eutectic composition agrees with the literature information quite well (x = of about 0.436, as estimated from the graphic form of the phase diagram), whereas our eutectic temperature is lower by 7 K. The effect in the solid phase was observed by us at temperature 603 K, and it was ascribed to decomposition of $NaNdBr_4$ compound into NaBr and $NdBr_3$ in the solid state. This compound has a completely different stoichiometry from that assumed in the literature [41], where it was defined as either Na_3NdBr_6 or Na_2NdBr_5. Additional thermal effect at 580 K, observed for the first time by us, was not reported in the literature.

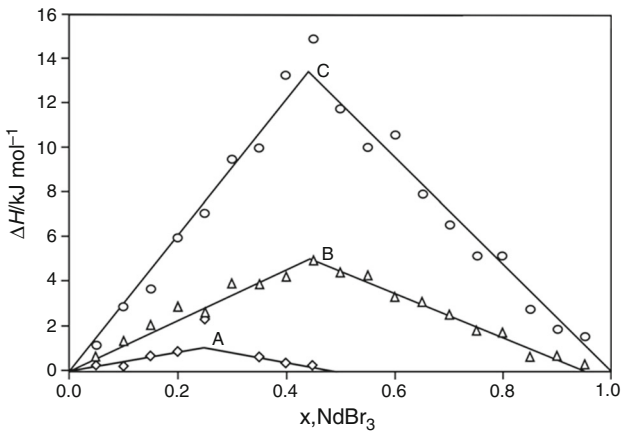

Fig. 2 Tammann diagram of $NdBr_3$–NaBr binary system: **a** decomposition of Na_3NdBr_6 compound; **b** decomposition of $NaNdBr_4$ compound; **c** $NdBr_3$–NaBr eutectic composition

Table 1 Results of the DSC experiments performed for the $NdBr_3$–NaBr binary system: T_1—decomposition of Na_3NdBr_6 in the solid state, T_2—decomposition of $NaNdBr_4$ in the solid state, T_3—temperature of NaBr–$NdBr_3$ eutectic

$X(NdBr_3)$	T_1/K	T_2/K	T_3/K	T_{Liq}/K
0.000	–	–	–	1022
0.050	580	599	636	994
0.100	581	603	654	964
0.150	582	604	641	917
0.200	580	605	640	856
0.250	582	606	635	818
0.300	579	605	651	732
0.350	580	606	646	696
0.400	580	606	638	–
0.450	580	605	645	681
0.500	–	602	646	732
0.551	–	602	645	774
0.600	–	602	643	812
0.650	–	602	642	806
0.700	–	601	645	859
0.751	–	599	643	879
0.798	–	605	643	903
0.849	–	602	661	917
0.900	–	602	640	938
0.950	–	602	637	949
1.000	–	–	–	954

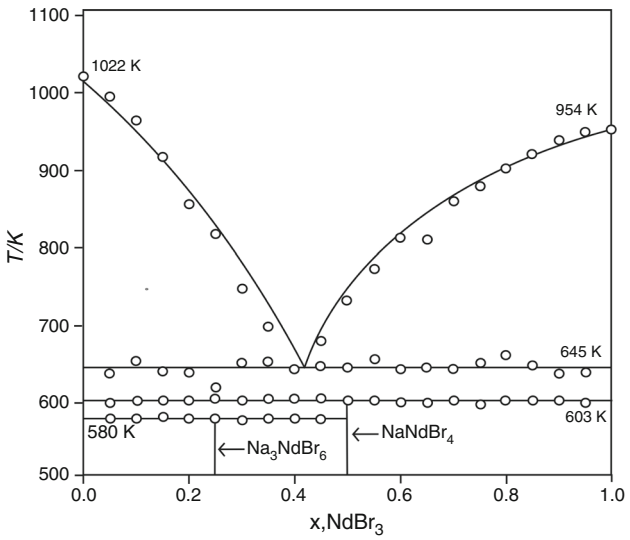

Fig. 3 Phase diagram of the $NdBr_3$–NaBr system

We could ascribe it to the Na_3NdBr_6 compound, which decomposes in the solid state into $NaNdBr_4$ and NaBr.

$NdBr_3$–KBr phase diagram

DSC investigations were performed for 28 samples with different compositions covering the entire composition range. The temperature and the fusion enthalpy of the related mixtures were obtained from the corresponding heating curves. Some characteristic DSC heating curves are presented in Fig. 4. The effects at the highest temperature are undoubtedly related to the liquidus temperatures. In the composition range $0 < x < 0.250$, where x is $NdBr_3$ mol fraction, two additional endothermic peaks were present in addition to the liquidus effect (Fig. 4a). The first one, observed in all the samples up to $x = 0.250$ at 849 K, can be undoubtedly ascribed to the KBr–K_3NdBr_6 eutectic. The eutectic composition, x ($NdBr_3$) = 0.192, was determined accurately from the Tammann plot presented in Fig. 5a, and the enthalpy of fusion at the eutectic composition is $\Delta_{fus}H_m$ = 13.6 kJ mol^{-1}. The second thermal effect, at 680 K (mean value from the measurements), was observable in all the curves up to $x = 0.333$, the composition at which it disappeared. This thermal effect corresponds to the formation of K_3NdBr_6 compound from MX and M_2LnX_5. The molar enthalpy related to this effect [calculated for K_3NdBr_6 compound (Fig. 5b)], $\Delta_{form}H_m$ = 45.8 kJ mol^{-1}, is in a good agreement with the enthalpy observed for the formation of many M_3LnX_6 compounds (M = alkali metal, Ln = lanthanide, X = halide) [42]. For the mixture with $x = 0.250$, only peaks at 683 and 918 K were observed in the curve (Fig. 4b). The latter peak has a typical shape of a congruently melting compound. We deduced that congruently melting K_3NdBr_6 compound exists in the $NdBr_3$–KBr system.

In the composition range $0.250 < x < 0.333$, two endothermic peaks were also present in addition to the liquidus effect (Fig. 4c). The first effect at 680 K (a mean value) agrees very well with effect observed for samples with molar fraction of NdBr3 $0 < x < 0.250$ and is undoubtedly related to formation of K_3NdBr_6 compound. Its disappearance at $x = 0.333$ suggests an existence of another compound, namely K_2NdBr_5. The second effect occurs at about 822 K in all the curves up to $x = 0.400$, the composition at which it disappeared. The Tammann diagram created for this effect (Fig. 5c) gives value $x = 0.325$, which is in an excellent agreement with the theoretical value 0.333 for K_2NdBr_5. Accordingly, the discussed effect can be ascribed to incongruent melting of K_2NdBr_5.

In the composition range $0.333 < x < 0.666$, only one endothermic peak at 754 K was observed, in addition to the liquidus, on the DSC curves (Fig. 4d). It disappears at $x = 0.666$, thus suggesting an existence of another compound, namely KNd_2Br_7, and can be ascribed to the K_2NdBr_5–KNd_2Br_7 eutectic. The K_2NdBr_5–KNd_2Br_7

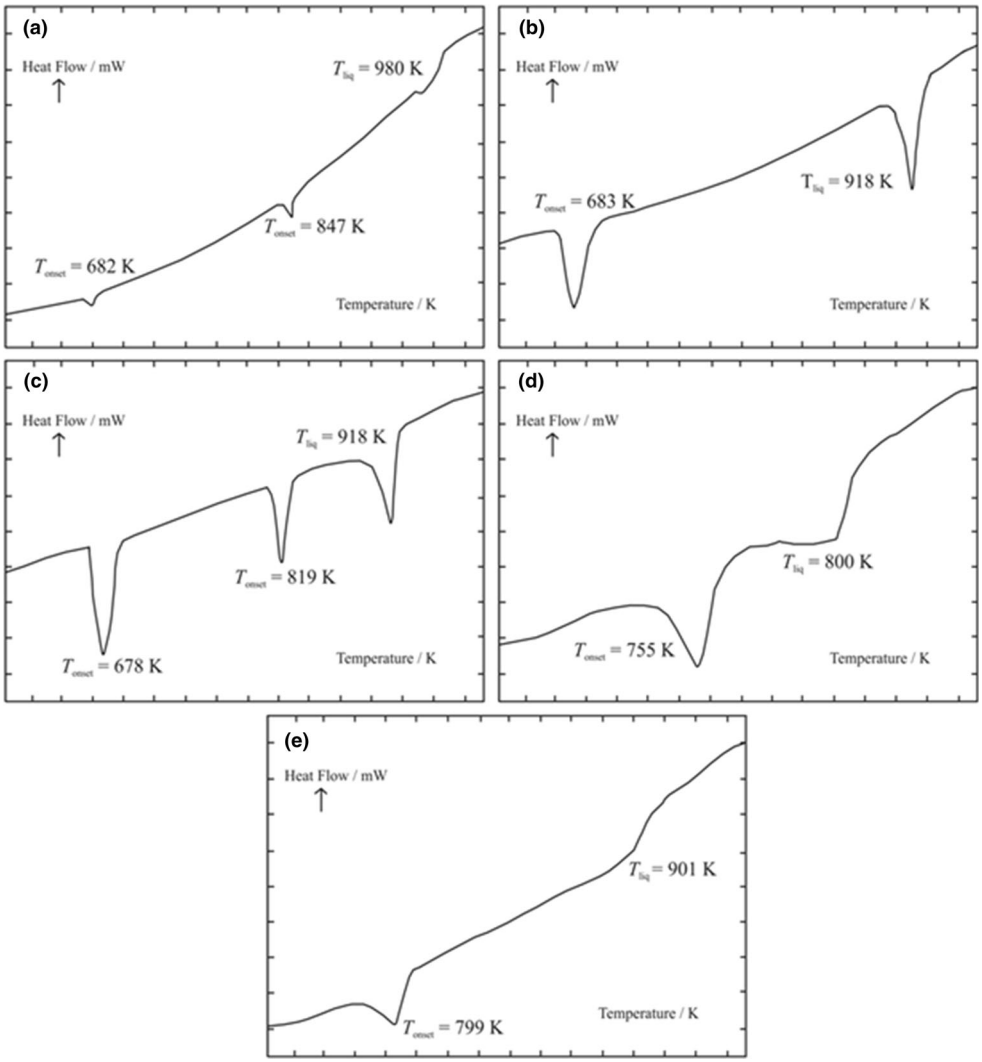

Fig. 4 DSC heating curves for KBr–$NdBr_3$ mixtures of different compositions: **a** x $NdBr_3$ = 0.051, **b** x $NdBr_3$ = 0.250, **c** x $NdBr_3$ = 0.270, **d** x $NdBr_3$ = 0.595, **e** x $NdBr_3$ = 0.850

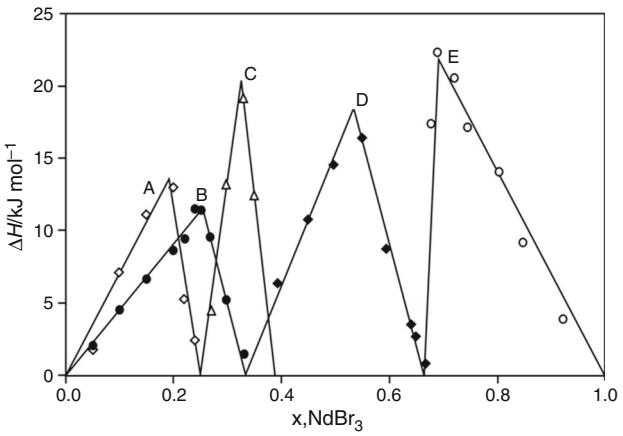

Fig. 5 Tammann diagram of $NdBr_3$–KBr binary system: determination of: **a** KBr–K_3NdBr_6 eutectic, **b** K_3NdBr_6 formation, **c** K_2NdBr_5 incongruent melting, **d** K_2NdBr_5–KNd_2Br_7 eutectic, **e** KNd_2Br_7–$NdBr_3$ eutectic

eutectic contribution to the enthalpy of fusion, determined and plotted versus the composition in Fig. 5d, gives the eutectic composition $x = 0.532$. The mixture with the eutectic composition melts with the enthalpy $\Delta_{fus}H_m$ of about 18.3 kJ mol^{-1}. In the composition range $0.666 < x < 1.0$, only one endothermic peak at 802 K was also observed in addition to the liquidus (Fig. 4e). It corresponds to the KNd_2Br_7–$NdBr_3$ eutectic. The eutectics composition $x = 0.689$ was determined from the intercept of the two linear parts in Fig. 5e. The corresponding enthalpy of fusion of the eutectic composition was found to be 21.7 kJ mol^{-1}. Analysis of the Tammann plots (Fig. 5) evidences that no solid solutions are formed in the system.

The complete $NdBr_3$–KBr phase diagram is presented in Fig. 6, and all the experimentally determined temperatures of thermal effects are presented in Table 2.

Our finding can be compared with the Gedlu et al.'s [23] as well as Blachnik and Jaeger-Kasper's [18] results. It is evident that Gedlu et al.'s [23] results are completely

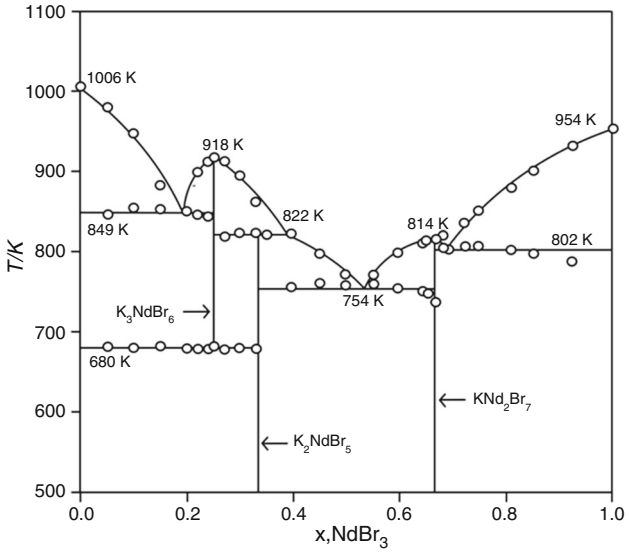

Fig. 6 Phase diagram of the $NdBr_3$–KBr system

wrong. Although they found two compounds of the same stoichiometry (K_3NdBr_6 and KNd_2Br_7), their properties are totally different. According to the authors [23], K_3NdBr_6 melts incongruently and KNd_2Br_7 decomposes in the solid state, whereas results of Blachnik and Jaeger-Kasper [18] as well as our findings indicate that these compounds melt congruently. In addition, Gedlu et al. [23] did not find another compound (K_2NdBr_5) in the system, whereas it was evidenced by Blachnik and Jaeger-Kasper [18] and by us. Our findings are comparable with Blachnik and Jaeger-Kasper's [18] results. Unfortunately, the latter are presented in a graphical form only. From this graphical presentation, the temperatures of characteristic points as well as eutectic compositions were estimated. The same defined compounds, namely K_3NdBr_6, K_2NdBr_5 and KNd_2Br_7, were found in the system. However, we found that K_3NdBr_6 was formed from KBr and K_2NdBr_5 at high temperature (683 K), whereas the literature [18] informs that it is not formation but a solid–solid transition. A significant difference was found in the melting temperature of K_3NdBr_6, K_2NdBr_5 and KNd_2Br_7 compounds. We determined these temperatures as 918 K, 822 and 814 K, respectively, whereas the literature data [18] (929, 828 and 835 K, respectively) are significantly higher. Significant differences were also found in the case of KBr–K_3NdBr_6, K_2NdBr_5–KNd_2Br_7 and KNd_2Br_7–$NdBr_3$ eutectics. Our finding for the eutectic temperatures (849, 754 and 802 K, respectively) is lower than those presented in the literature [18] (861, 758 and 809 K, respectively). Moreover, our finding for the eutectics compositions (x ($NdBr_3$) = 0.192, 0.532 and 0.689, respectively) differs from those found in the literature data [18] (x ($NdBr_3$) = 0.177, 0.558 and 0.699, respectively).

Table 2 Results of the DSC experiments performed for the $NdBr_3$–KBr binary system: T_1—formation temperature of K_3NdBr_6, T_2—KBr–K_3NdBr_6 eutectic temperature, T_3—temperature of incongruent melting of K_2NdBr_5, T_4—K_2NdBr_5–KNd_2Br_7 eutectic temperature, T_5—KNd_2Br_7–$NdBr_3$ eutectic temperature

$X(NdBr_3)$	T_1/K	T_2/K	T_3/K	T_4/K	T_5/K	$T_{liquidus}$/K
0.000	–	–	–	–	–	1006
0.051	682	847	–	–	–	980
0.099	680	855	–	–	–	947
0.149	682	852	–	–	–	883
0.199	680	851	–	–	–	–
0.220	679	846	–	–	–	899
0.240	679	844	–	–	–	914
0.250	683	–	–	–	–	918
0.270	678	–	819	–	–	913
0.298	680	–	824	–	–	895
0.329	680	–	824	–	–	863
0.350	–	–	822	–	–	–
0.396	–	–	–	756	–	822
0.449	–	–	–	761	–	798
0.497	–	–	–	759	–	772
0.550	–	–	–	760	–	772
0.595	–	–	–	755	–	800
0.643	–	–	–	751	–	812
0.650	–	–	–	750	–	814
0.667	–	–	–	738	–	814
0.680	–	–	–	–	805	820
0.692	–	–	–	–	804	–
0.721	–	–	–	–	807	836
0.747	–	–	–	–	807	851
0.807	–	–	–	–	802	880
0.850	–	–	–	–	799	901
0.924	–	–	–	–	787	933
1.000	–	–	–	–	–	954

Conclusions

1. Phase equilibria in the $NdBr_3$–MBr binary systems (M = Na, K) were established by differential scanning calorimetry (DSC). The system with NaBr is a simple eutectic system with two compounds that decompose in the solid state ($NaNdBr_4$ at 603 K and Na_3NdBr_6 at 580 K). In the system with KBr, three stoichiometric compounds exist. First (K_3NdBr_6) is formed from KBr and K_2NdBr_5 at 680 K and melts congruently at 918 K. Second (KNd_2Br_7) melts congruently at 814 K. Third compound (K_2NdBr_5) melts incongruently at 822 K.
2. The composition of the eutectics was determined with the help of constructed Tammann diagrams. NaBr–

$NdBr_3$, KBr–K_3NdBr_6, K_2NdBr_5–KNd_2Br_7 and KNd_2Br_7–$NdBr_3$ eutectics were found to be located at x = 0.443 (644 K), 0.192 (849 K), 0.532 (754 K) and 0.689 (802 K), respectively.

3. Literature data on the systems under investigation were verified, and some of them were found to be completely wrong.

Acknowledgements The work was financed by a statutory activity subsidy from the Polish Ministry of Science and Higher Education for the Faculty of Chemistry of Wroclaw University of Science and Technology. Financial support by the Algerian Ministry of Higher Education and Scientific Research is gratefully acknowledged. M. B and Y. B wish to thank the Department of Chemistry of Wroclaw University of Science and Technology for the hospitality and support during this work.

References

1. Markus T, Ohnesorge M, Mollenhoff M, Hilpert K. Aspects of high temperature chemistry in metal halide lamps. In: Taxil P, Bessada C, Cassir M, Gaune-Escard M (eds) Proceedings of the 7th international symposium on molten salts chemistry and technology. Toulouse, France; 2005. p. 743–6.
2. Mucklejohn SA, Dinsdale AT. The behaviour of metal halide systems in high intensity discharge lamps. In: Taxil P, Bessada C, Cassir M, Gaune-Escard M, editors. Proceedings of the 7th international symposium on molten salts chemistry and technology. Toulouse, France; 2005. p. 761–4.
3. Guest EC, Mucklejohn SA, Preston B, Rouffet JB, Zissis G. ''NumeLiTe'': an energy effective lighting system for roadways and an industrial application of molten salts. In: Oye HA, Jagtoyen A, editors.Proceedings of international symposium on ionic liquids in honour of M. Gaune-Escard. France; 2003. pp. 37–45.
4. Van Erk W. Transport processes in metal halide discharge lamps. Pure Appl Chem. 2000;72:2159–66.
5. Mucklejohn SA, Trindell D, Devonshire R. An assessment of the thermochemical parameters for the lanthanide triiodides. Presented as a poster paper 37P at: the 6th international symposium on science & technol. Light Sources, Budapest, Hungary; 1992.
6. Brumleve TR, Voggenauer K, Lovell ME, Scott TE, DeHaven DB, Gordon D, Steward RL, Hansen SC. Spectra of rare-earth iodide-cesium iodide systems in low-wattage metal halide lamp. In: Proceedings of the 11th international symposium on the science and technology of light sources. China; 2007. Paper CP090.
7. Kirby MW. Mercury lamps. In: Coaton JR, Marsden AM, editors.Lamps and lighting. 4th ed. London; 1997. p. 227–62.
8. Preston B, Odel EC. Metal halide lamps. In: Coaton JR, Marsden AM, editors. Lamps and lighting. 4th ed. London; 1997. p. 263–80.
9. Mucklejohn SA. Molten salt high-intensity discharge lamps. In: Proceedings of the international George Papatheodorou symposium. Patras; 1999. p. 63–7.
10. Edgar A, Williams GVM, Appleby GA. Photo-stimulated luminescence from europium-doped rubidium barium bromide in fluorozirconate glass ceramics. J Lumin. 2004;108:19–23.
11. Rademaker K, Heumann Huber EG, Payne SA, Krupke WF, Isaenko LI, Burger A. Laser activity at 1.18, 1.07, and 0.97 microm in the low-phonon-energy hosts KPb2Br 5 and RbPb2Br5 doped with Nd3+. Opt Lett. 2005;7:729–31.
12. Rademaker K, Payne SA, Huber G, Isaenko LI, Osiac E. Optical pump–probe processes in Nd3 + -doped KPb2Br 5, RbPb2Br5, and KPb2Cl5. J Opt Soc Am B. 2005;22:2610–8.
13. Oron R, Bunimovich D, Nagli L, Katzir A. Design considerations for rare earth doped silver halide fiber amplifiers. Opt Eng. 2001;40:1516–20.
14. Bessiere A, Dorenbos P, Van Eijk CWE, Kramer KW, Gudel HU, Galtayries A. Scintillation and anomalous emission in elpasolite $Cs_2LiLuCl_6$:Ce^{3+}. J Lumin. 2006;117:187–98.
15. Naqvi AA, Khiari FZ, Maslehuddin M, Gondal MA, Al-Amoudi OSB, Ukashat AM, Ilyas MS, Liadi FA, Isab AA, Rehman K, Raashid M, Dastageer MA. Pulse height tests of a large diameter fast LaBr 3: Ce scintillation detector. Appl Radiat Isot. 2015;104:224–31.
16. Konings RMJ, Kvacs A. Handbook on physics and chemistry of rare earths. In: Gschneider KA, Bunzli JCG, Pecharsky VK, editors. Elsevier, Amsterdam; 2003.
17. Vogel G. Untersuchung der Zustandsdiagramme von Lanthanidenbromiden mit Alkalibromiden. Z Anorg Allg Chem. 1972;388:43–52.
18. Blachnik R, Jaeger-Kasper A. Zustandsdiagramme von alkalibromid-lanthanoid(III)-bromid mischungen. Z Anorg Allg Chem. 1980;461:74–86.
19. Molodkin AK, Strekachinskii AB, Dudareva AG, Ezhov AI, Krokhina AG. Wzaimodejstvije bromida tulia z bromidami natrija, kalija i cezija. Zh Neorg Khim. 1982;27:219–22.
20. Molodkin AK, Strekachinskii AB, Dudareva AG. Systema TmBr3–LiBr. Zh Neorg Khim. 1982;27:261–3.
21. Molodkin AK, Karagodina AM, Dudareva AG, Strekachinskii AB. Systema TmBr3–RbBr. Zh Neorg Khim. 1981;26:2265–7.
22. Seifert HJ, Yuan Y. Thermochemical studies on the systems ABr–LaBr 3 (A ≡ Na, K, Rb, Cs). J Less-Common Met. 1991;170:135–43.
23. Gedlu TA, Dudareva AG, Kartashova IW. Physiko—khimicheskije izutschenije diagrammy sostojania sistemy NdBr3–MBr (M = K, Rb). Zh Prikl Khim. 1993;66:1861–3.
24. Ingier-Stocka E, Rycerz L, Gadzuric S, Gaune-Escard M. Thermal and conductometric studies of the $CeBr_3$–LiBr binary system. In: Proceedings of the 7th international symposium on molten salts chemistry and technology, MS 7, Toulouse, France; 2005. p. 829–831.
25. Ingier-Stocka E, Rycerz L, Gadzuric S, Gaune-Escard M. Thermal and conductometric studies of the CeBr3–MBr binary systems (M = Li, Na). J. Alloys Compd. 2008;450:162–6.
26. Rycerz L, Ingier-Stocka E, Gadzuric S, Gaune-Escard M. Phase diagram and electrical conductivity of CeBr3–KBr. Z Naturforsch. 2007;62a:197–204.
27. Rycerz L, Ingier-Stocka E, Gadzuric S, Gaune-Escard M. Phase diagram and electrical conductivity of the CeBr 3–RbBr binary system. J Alloys Compd. 2008;450:175–80.
28. Rycerz L, Ingier-Stocka E, Gaune-Escard M. Phase diagram and electrical, conductivity of the CeBr3–CsBr binary system. J Therm Anal Calorim. 2009;97:1015–21.
29. Ingier-Stocka E, Rycerz L, Berkani M, Gaune-Escard M. Thermodynamic and transport properties of the PrBr 3–MBr binary systems (M = Li, Na). J Mol Liq. 2009;148:40–4.
30. Rejek J, Rycerz L, Ingier-Stocka E, Gaune-Escard M. Thermodynamic and transport properties of the PrBr 3 − KBr binary system. J Chem Eng Data. 2010;55:1871–5.

31. Rycerz L, Ingier-Stocka E, Berkani M, Gaune-Escard M. Thermodynamic and transport properties of the PrBr 3–RbBr binary system. J Alloys Compd. 2010;501:269–74.
32. Rycerz L, Ingier-Stocka E, Berkani M, Gaune-Escard M. Phase diagram and electrical conductivity of the PrBr 3–CsBr binary system. Z Naturforsch. 2010;65a:859–64.
33. Rycerz L, Gong W, Gaune-Escard M. The TbBr 3–LiBr binary system: experimental thermodynamic investigation and assessment of phase diagram. J Chem Thermodyn. 2013;56:15–20.
34. Rycerz L, Gaune-Escard M. Phase diagram of the TbBr3–RbBr binary system: thermodynamic and transport properties of the Rb3TbBr6 compound. Inorg Chem. 2007;46:2299–306.
35. Rycerz L, Chojnacka I, Kapala J, Gaune-Escard M. Phase diagram of the TbBr3–CsBr binary system. thermodynamic and transport properties of the Cs3TbBr6 compound. Calphad. 2012;37:108–15.
36. Kubikova B, Rycerz L, Chojnacka I, Gaune-Escard M. Thermodynamic and transport properties of the DyBr3–LiBr binary system. J Phase Equillib Diffus. 2009;30:502–8.
37. Chojnacka I, Rycerz L, Berkani M, Gaune-Escard M. Phase diagram and electrical conductivity of the DyBr3–RbBr binary system. J Therm Anal Calorim. 2012;108:481–8.
38. Chojnacka I, Rycerz L, Berkani M, Gaune-Escard M. Phase diagram and electrical conductivity of the DyBr3–CsBr binary system. J Alloys Compd. 2014;582:505–10.
39. Chojnacka I, Rycerz L, Gaune-Escard M. Thermodynamic and transport properties of the DyBr3–NaBr binary system. J Therm Anal Calorim. 2014;116:681–7.
40. Berkani M, Bounouri Y, Gaune-Escard M. Phase diagram and electrical conductivity of $NdBr_3$–KBr. In: Kongoli F, Gaune-Escard M, Turna T, Mauntz M, Dods HL, editors. SIPS 2016, Volume 9: Molten salts and ionic liquids, energy production. FLOGEN star outreach, Montreal, Canada, 2016. p. 197–198.
41. Szczygieł I, Salamon B, Kapała J. Modelling of thermodynamic properties of NdBr3–MBr (M = Li–Cs) pseudobinary systems. Calphad. 2016;53:130–5.
42. Rycerz L. High temperature characterization of LnX_3 and LnX_3–AX solid and liquid. Systems (Ln = Lanthanide, A = Alkali, X = Halide): thermodynamics and electrical. Conductivity. Ph.D. thesis, Université de Provence Aix-Marseille I, France, Marseille, 2003.